

An Animal Model of Colorectal Cancer Liver Metastasis With a High Metastasis Rate and Clonal Dynamics

KI BEOM BAE^{1,2}, SUN-HEE KIM^{1,2,3}, MI SEON KANG⁴ and DONG-HYUN KIM⁵

¹Department of Surgery, Busan Paik Hospital, Inje University College of Medicine, Busan, Republic of Korea;

²Paik Institute for Clinical Research, Inje University College of Medicine, Busan, Republic of Korea;

³In-Dang Bio Medical Research Institute, Busan Paik Hospital, Inje University College of Medicine, Busan, Republic of Korea;

⁴Department of Pathology, Busan Paik Hospital, Inje University College of Medicine, Busan, Republic of Korea;

⁵Department of Pharmacology, Busan Paik Hospital, Inje University College of Medicine, Busan, Republic of Korea

Abstract. *Background:* Various animal models have been introduced into the study of liver metastasis of colorectal cancer, but they have not been compared under the same conditions. The aim of this study was to identify an optimized mouse model that showed a high rate of hepatic metastasis and expression of clonal dynamics. *Materials and Methods:* Athymic nude mice ($n=30$) were divided into two equal groups for the creation of a splenic injection model (SIM) and surgically orthotopic implantation model (SOIM) of liver metastasis of colorectal cancer using HCT116 cells. Hepatic metastasis was confirmed by gross and microscopic examinations. Expression of MET transcriptional regulator MACC1 (MACC1) in colon cancer cell lines and metastatic tumors in the group with a higher liver metastasis rate was confirmed by quantitative reverse-transcription–polymerase chain reaction. *Results:* The observation time was significantly shorter for SIM than for SOIM (33.0 ± 6.8 vs. 41.2 ± 7.2 days, $p<0.001$). The rate of hepatic metastasis was significantly higher in SIM than in SOIM (76.9% vs. 38.4%, $p=0.038$). MACC1 was expressed in Colo201, HCT116, HT29, LS513, SW620, and WiDr cells but not in SW480 cells. All hepatic metastases in SIM mice expressed MACC1, and metastatic HCT116 cells had significantly greater expression than did the original HCT116 cells ($p<0.001$). *Conclusion:* With a higher rate of hepatic metastasis with clonal dynamics in a shorter observation time than the SOIM, SIM appears to be a good animal model for

identifying new targets and in drug development for colorectal cancer liver metastasis. SOIM should also be considered for the study of the full steps of metastasis.

Colorectal cancer (CRC) is currently the third leading cause of death in the United States, and its incidence is increasing in Asia. The main cause of death from CRC is metastasis (1). Approximately 70-80% of CRC metastases occur in the liver (2). Genes and other factors that affect the adenoma–carcinoma sequence and the onset of CRC have been well established but those affecting CRC metastasis remain unclear (3). Anticancer chemicals and monoclonal antibody therapies that suppress metastasis and recurrence are being used to treat diseases (4-7). Notably, these drugs only suppress cell division and growth. Currently, no drug is available that definitively blocks the process of metastasis. There is a strong need to determine the causative biomarkers of metastasis, particularly liver metastasis. Patient-derived xenograft (PDX) models generated by direct engraftment of human tumor tissues obtained through biopsy or surgical resection into immunodeficient rodents are the models of choice for the investigation of clinically relevant questions in cancer research (8). The subcutaneous injection method is suitable for the observation of cancer growth rates and for drug-screening tests. However, liver metastasis does not occur by this method (9-11). The intraportal injection method reproducibly results in liver metastasis in almost all animals but mortality rates due to surgery or anesthesia are 6-10% and the method is more complicated than the splenic injection method (12, 13). The surgical orthotopic implantation model (SOIM), which offers the advantage of microenvironment maintenance for study of the metastatic capacity of tumor cells (14), and the splenic injection model (SIM) are both suitable for the modeling of hematogenous metastasis (10, 13). Although several studies of the SOIM and SIM have been conducted, these models have not been compared

Correspondence to: Ki Beom Bae, Department of Surgery, Busan Paik Hospital, Inje University College of Medicine, Busan 47392, Republic of Korea. Tel: +82 518906075, Fax: +82 518909427, e-mail: bkbsur@yahoo.co.kr

Key Words: Colorectal cancer, liver metastasis, clonal dynamics, animal model, splenic injection, orthotopic implantation.

directly as far as we are aware. Furthermore, these animal models yield different metastatic rates depending on the mouse strain, cancer cell line, and injection method used, which impedes selection of a suitable animal model for the study of liver metastasis. Another critical consideration is that cancer evolves by a reiterative process of clonal expansion, genetic diversification and clonal selection (15). Although PDXs can largely recapitulate the polygenomic architecture of human tumors, they do not fully account for heterogeneity in the tumor microenvironment (16). Human tumors are comprised of multiple subclones that harbor distinct genetic and epigenetic changes. The ideal animal model should reflect heterogeneity and clonal dynamics. Thus, an optimized mouse model with a high metastatic rate, simple method of generation, short observation time, high degree of reproducibility, and clonal dynamics must be established preferentially for the study of liver metastasis of CRC.

The aim of this study was to identify an optimized mouse model with an improved rate of hepatic metastasis and clonal dynamics by comparing the SIM and SOIM under the same experimental conditions.

Materials and Methods

Athymic nude mice (n=30) were divided into two equal groups for creation of the SIM and SOIM. The metastatic rate was determined according to the prevalence of metastases on gross and microscopic examination. All experiments were conducted after obtaining approval from the Inje University College of Medicine Animal Ethics Committee (no. 2017-013).

Cell lines and culture. Colon cancer cell lines Colo201, HCT116, HT29, LS513, SW480, SW620 and WiDr were purchased from the American Type Culture Collection (Manassas, VA, USA). The cells were cultured in RPMI 1640 medium supplemented with 5% fetal bovine serum and glutamine. HCT116 cells are poorly differentiated CRC cells that secrete 1 ng carcinoembryonic antigen per million cells; they were originally isolated from a 50-year-old male patient. The HCT116 cell line was chosen to compare the animal models because it is a well-known colon cancer cell line with high tumor take and metastasis rates (17, 18). A total of 2×10^6 HCT116 cells per 100 μ l RPMI 1640 medium were used for the SIM. A total of 5×10^6 HCT116 cells per 200 μ l RPMI 1640 medium were used to produce xenografts for the SOIM.

Mice. Female BALB/c athymic nude mice aged 6 weeks (Orient Co., Seoul, Korea) with a mean body weight of 18.5 ± 0.8 g were used. Fifteen mice were assigned to each of the SIM and SOIM groups. They were kept in cages (three mice/cage) with free access to food and water, and a 12/12-h light/dark cycle.

Splenic injection. The athymic nude mice were anesthetized with 2% isoflurane. All surgeries were performed with the mouse on a heating pad equipped with a thermometer to maintain the animal's body temperature during the procedure. Each mouse was placed on the operating table in the right lateral recumbent position, and the skin was sterilized using 83% alcohol swabs. A left-side flank

incision was made, and the peritoneum was opened to a length of approximately 8 mm; the spleen was exposed over the peritoneum. HCT116 cells ($2 \times 10^6/100$ μ l) were injected slowly into the splenic parenchyma using a 30-G needle (Figure 1). Then the puncture site was pressed closed with a cotton swab for 10 min to prevent bleeding and cell leakage. After confirming the lack of bleeding at the injection site, the spleen was returned to the abdominal cavity, and the peritoneum was closed in one layer using 4-0 absorbable Vicryl sutures. The mice were kept in the recovery room on heating pads to maintain their body temperatures until they recovered from anesthesia. They were then returned to their cages.

Surgical orthotopic implantation. HCT116 cells ($5 \times 10^6/200$ μ l) were injected into the subcutaneous layers of both flanks of five athymic nude mice to establish a subcutaneous xenograft. Once the size of the xenograft tumor exceeded 1 cm, after 2-6 weeks, the mice were euthanized, and the tumors were removed and stored in Earle's minimum essential medium at 4°C. Before implantation, each xenograft tumor was washed twice with antibiotic-containing Earle's minimum essential medium for at least 10 min to prevent contamination and infection. After the removal of necrotic and noncancerous tissues of the xenograft tumor, the remaining cancer tissues were divided into pieces of approximately 1 mm³. A 1-cm midline laparotomy was performed in a healthy nude mouse under 2% isoflurane anesthesia for orthotopic implantation of these small pieces of xenograft. The cecum was exteriorized, and the colonic subserosal layer was exposed by tearing the serosa with two sharp microforceps. Two 1-mm³ pieces of xenograft tumor were implanted into the mural wall at two different sites using 9-0 nonresorbable sutures under a dissecting microscope. The cecum was returned to the abdominal cavity, and the laparotomy was closed using 4-0 absorbable Vicryl sutures. A schematic illustration of the SOIM procedure is provided in Figure 2.

Gross and microscopic assessment. The mice were monitored closely until 20-30% of all mice in each group showed cachexia. At this time, the mice were euthanized with CO₂ gas, and necropsy was initiated. The liver, lymph nodes, lung, peritoneum, and spleen of each mouse were resected and processed for gross and microscopic examinations. Portions of the harvested organs were fixed in 10% neutral buffered formalin for 24 h and embedded in paraffin. The tissues were stained with hematoxylin and eosin. A pathologist assessed metastasis grossly and microscopically in a double-blinded manner.

Quantitative reverse-transcription polymerase chain reaction. Expression of the MET transcriptional regulator MACC1 (*MACC1*) gene was analyzed to identify the clonal dynamics of the metastatic tumors compared with the original cancer cells. The colon cancer cell lines and samples of tumor metastases in the group with the highest metastasis rates were selected, and mRNA was obtained using a total RNA extraction kit (Easy-Spin; iNtRON Biotechnology, Daejeon, Republic of Korea). For quantitative reverse-transcription polymerase chain reaction (qRT-PCR), 5 μ g Oligo(dT) primer (Promega, Madison, WI, USA) was added to 1 μ g total RNA in a total volume of 15 μ l in nuclease-free water, and incubated at 70°C for 10 min. The RNA template was incubated at 42°C for 1 h and 72°C for 10 min with a mixture that included M-MLV reverse transcriptase (Promega) for cDNA synthesis. Next, the synthesized cDNA template was added to the qRT-PCR reaction

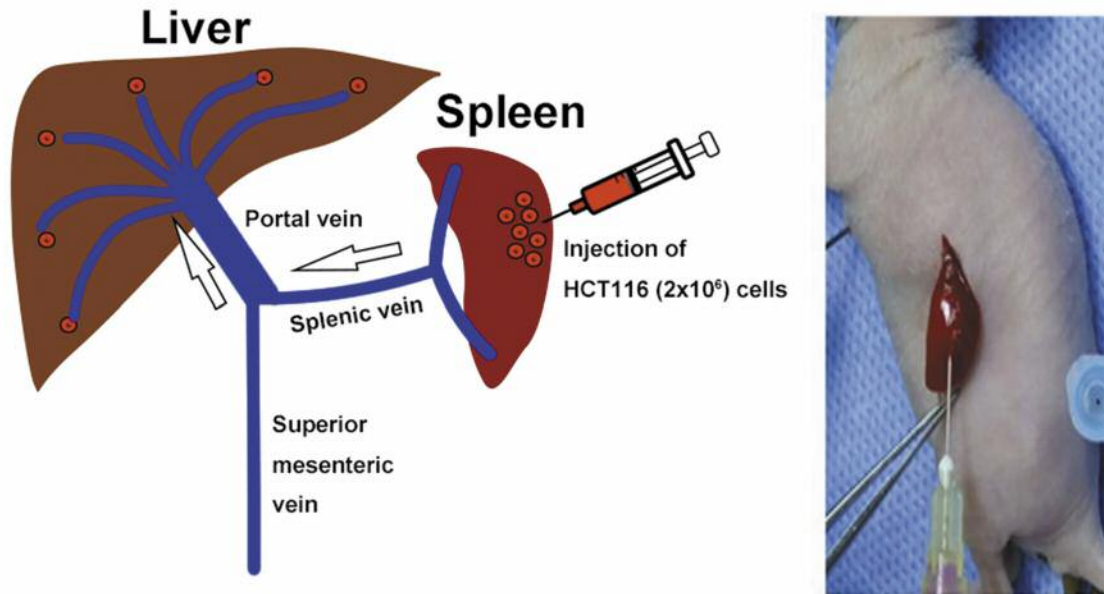


Figure 1. Splenic injection model with HCT116 cells. In total, $2 \times 10^6 / 100 \mu\text{l}$ HCT116 cells were injected slowly into the splenic parenchyma using a 30-G needle. The puncture site was pressed closed with a cotton swab for 10 min to prevent bleeding and cell leakage.

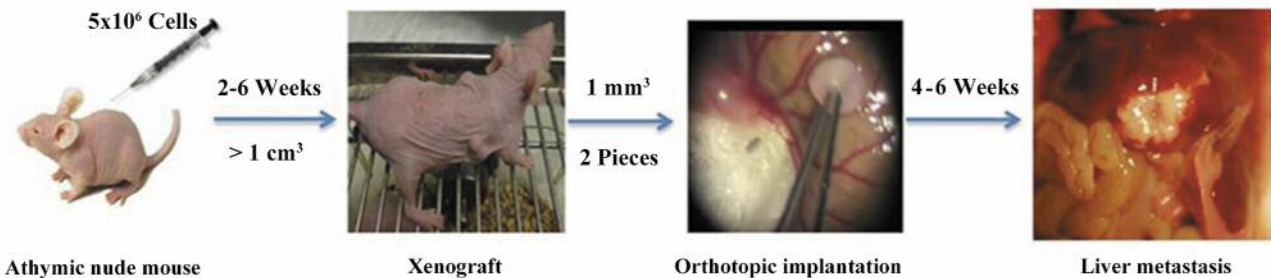


Figure 2. Surgical orthotopic implantation model with HCT116 xenograft. Small pieces of tumor from a 1-cm xenograft developed from subcutaneous injection of 5×10^6 HCT116 cells were orthotopically implanted into the subserosal layer of the cecum in each healthy nude mouse using a dissecting microscope.

mixture, and qRT-PCR was performed. The *MACC1* primer sequences were: forward, 5'-TTCTTTTGATTCCTCCGGTGA-3' and reverse, 5'-ACTCTGATGGGCATGTGCTG-3'. PCR consisted of 35 total cycles of 30 s at 95°C for pre-denaturation, 5 s at 95°C for denaturation, 40 s at 55°C for annealing, 30 s of extension at 72°C, and 10 min for the last extension at 72°C. Glyceraldehyde 3-phosphate dehydrogenase (*GAPDH*) mRNA was used as an internal control. The *GAPDH* primer sequences were: forward, 5'-GAAGATGGTGATGGGATTTC-3' and reverse, 5'-GAAGGTGAAGGTCGGAGT-3'. All PCR samples were assessed by 2% agarose gel electrophoresis. The ratio of *MACC1* expression relative to that of *GAPDH* was quantified with using Image J (National Institutes of Health, Bethesda, MA, USA).

Western blot analysis. The extraction of proteins from each colon cancer cell lines and metastatic liver tumors were performed with Pro-Prep solution (iNtRON Biotechnology, Daejeon, Republic of Korea) containing a phosphatase inhibitor cocktail (Sigma, Saint

Louis, MO, USA). After lysis, protein quantification was performed using Bradford assays (Biorad, Hercules, CA, USA). The samples were electrophoresed by 10% sodium dodecyl sulfate - polyacrylamide gel electrophoresis gel (30 mA for 2 h) and transferred onto polyvinylidene fluoride membrane (400 mA for 2 h, at 4°C). After probing with 1:1000 diluted rabbit polyclonal antibody to *MACC1* (Abcam, Cambridge, MA, USA) at 4°C overnight, the blots were subsequently incubated with horseradish peroxidase-conjugated secondary antibody (1:5,000). The blots were visualized using ECL system (Amersham Biosciences, Cambridge, UK) and LAS3000 (Fuji Film, Tokyo, Japan).

Immunohistochemistry. Metastatic tumors in liver were prepared for immunohistochemistry from the formalin-fixed paraffin-embedded tissues from harvested mouse liver. The specimens were sliced at 4- μm thickness, deparaffinized, and then rehydrated in graded alcohols. Immunohistochemical staining for *MACC1* was performed

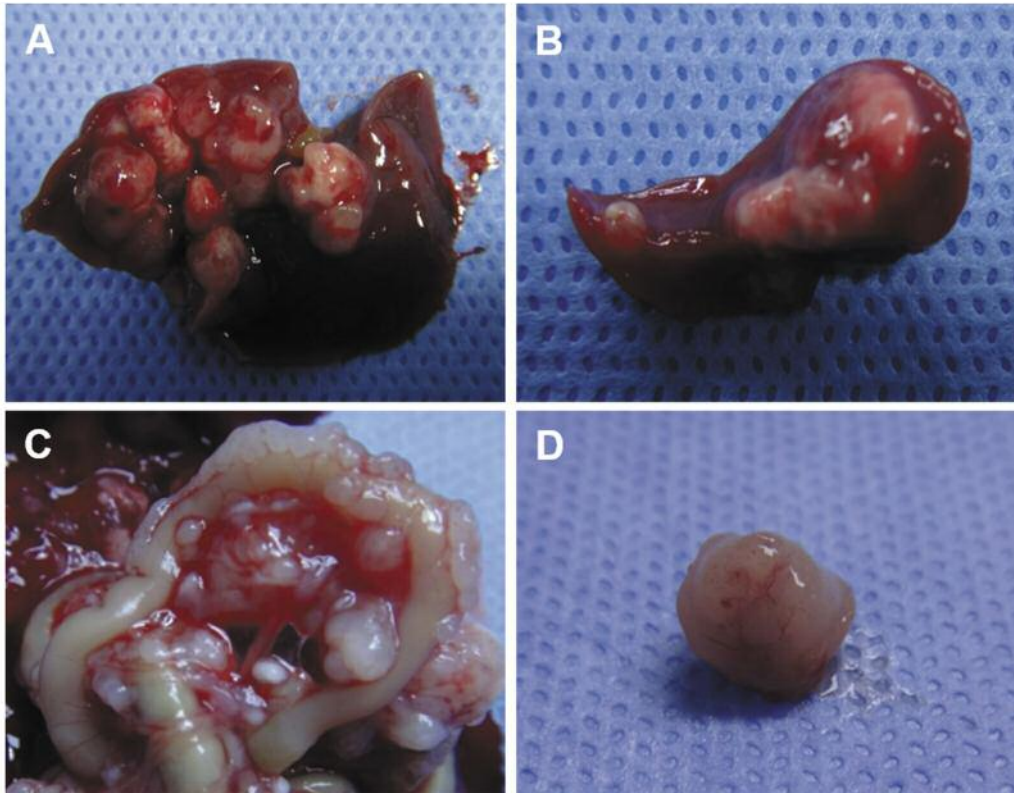


Figure 3. Gross findings for the splenic injection model. A: Numerous whitish metastatic nodules were seen in the liver parenchyma. B: Spleen with a successfully implanted tumor and a whitish mass. C: Peritoneal seeding. D: Axillary lymph-node enlargement with tumor metastasis.

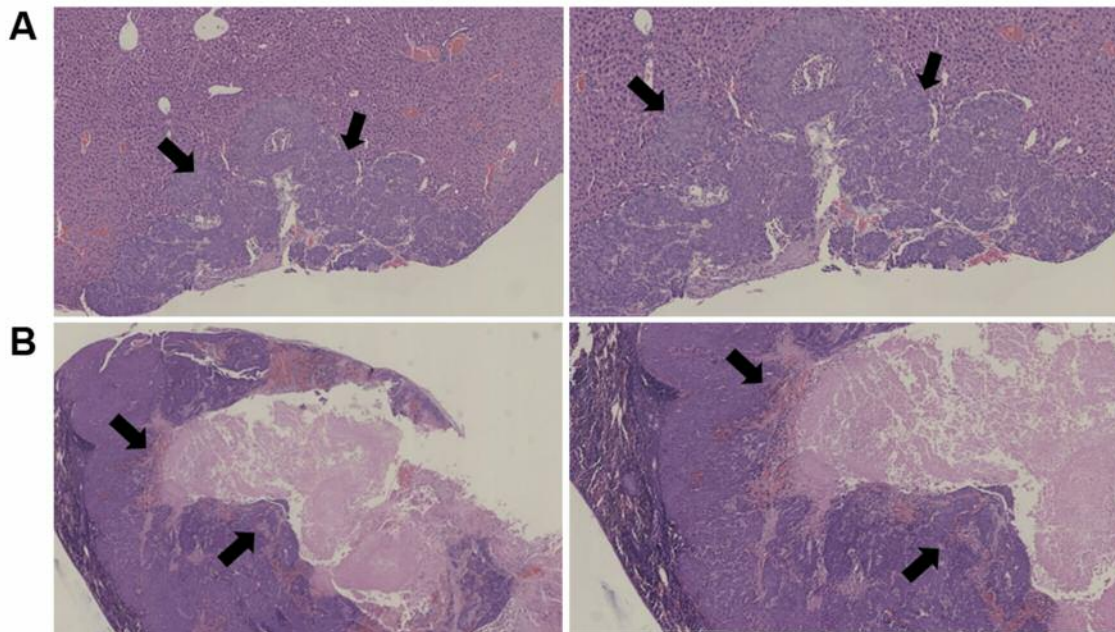


Figure 4. Microscopic findings for the splenic injection model at $\times 20$ (left panels) and $\times 40$ (right panels) as shown by hematoxylin and eosin staining. A: Metastatic carcinoma (arrows) was seen in the liver. B: The spleen was infiltrated by implanted HCT116 cancer cells, with central tumor necrosis (arrows).

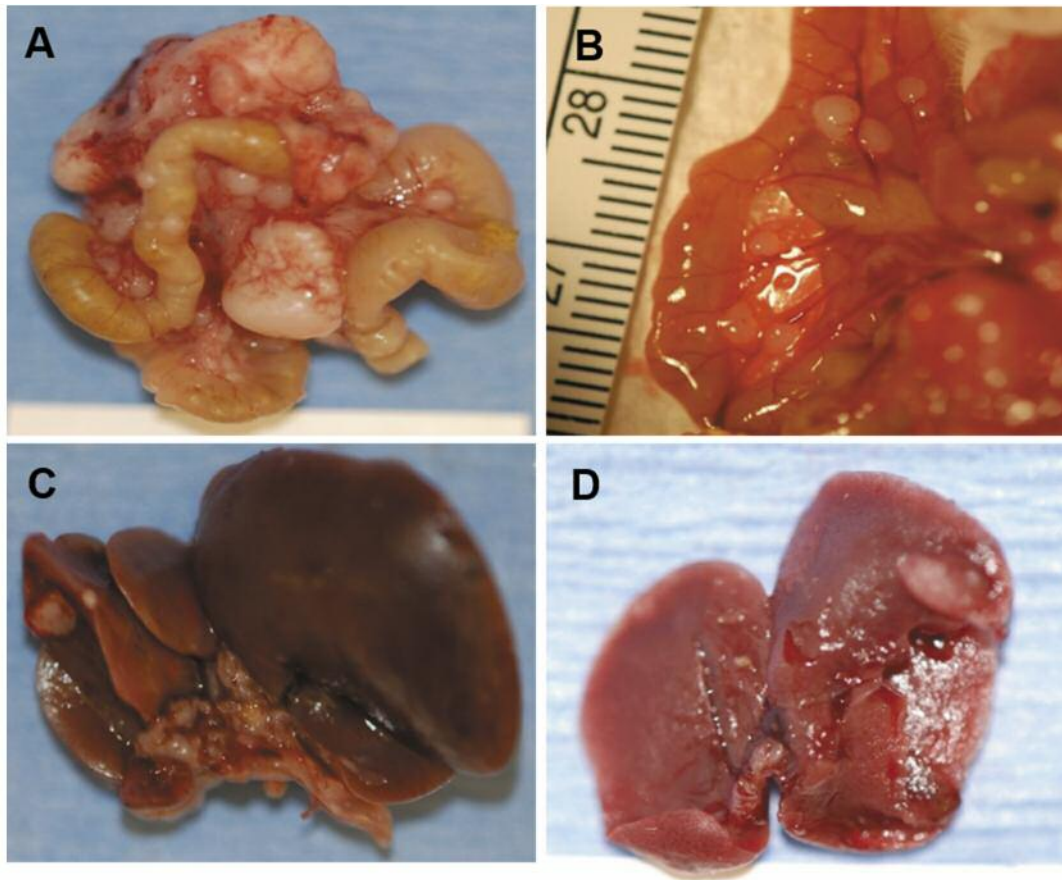


Figure 5. Gross findings for the surgical orthotopic implantation model. A: Orthotopically implanted tumors successfully grew and formed a huge conglomerated mass in the colon. B: Peritoneal seeding. C: Whitish metastatic nodules were detected in the liver. D: Whitish nodular metastatic lesions were detected in the lungs.

using the avidin–biotin–peroxidase complex method, with primary reaction with rabbit polyclonal MACC1 antibody (Abcam). As secondary antibody, anti-rabbit horseradish peroxidase-conjugated was used according to the manufacturer's protocol.

Statistical analysis. The statistical analysis was performed using SPSS 21.0 for Windows (IBM, Armonk, NY, USA). The chi-squared test was used to assess categorical variables. Mean differences between two independent groups were analyzed using Student's *t*-test. *p*-Values of less than 0.05 were considered to be significant.

Results

Comparison of the SIM and SOIM. Two mortalities were recorded, one from each mouse group; these mice did not recover from anesthesia. The mean observation times for the SIM and SOIM groups ($n=14$ each) were 33.0 ± 6.8 and 41.2 ± 7.2 days, respectively ($p<0.001$). The rate of survival of implanted tumor in mice, which included growth at the local implantation site, peritoneal seeding/liver metastasis, was the same for both groups (13/14). The rates of tumor growth at the implantation sites were 10/13 in the SIM group

and 13/13 in the SOIM group ($p=0.065$). Peritoneal seeding did not differ between groups (9/13 vs. 9/13), but the liver metastasis rate was significantly higher in the SIM group than in the SOIM group (10/13 vs. 5/13, $p=0.038$). Gross examination of samples from the SIM group showed whitish splenic lesions in the HCT116-implanted parenchyma and multiple nodular whitish metastases in the livers, which seemed to be shaped very similarly to human liver metastases of CRC (Figure 3A and B). Peritoneal seeding was detected in the whole abdomen, and in the mesentery and bowel walls (Figure 3C). Axillary lymph-node metastasis, which is not a common growth pattern of human CRC, was noted in two mice of the SIM group (Figure 3D). Microscopic examination of samples from the SIM group showed that pleomorphic and hyperchromatic metastatic carcinoma cells had infiltrated the mouse liver parenchyma (Figure 4A), and the spleen was infiltrated by the implanted HCT116 cancer cells with central tumor necrosis (Figure 4B). Gross examination of samples from the SOIM group revealed a huge conglomerated mass growing on the colon

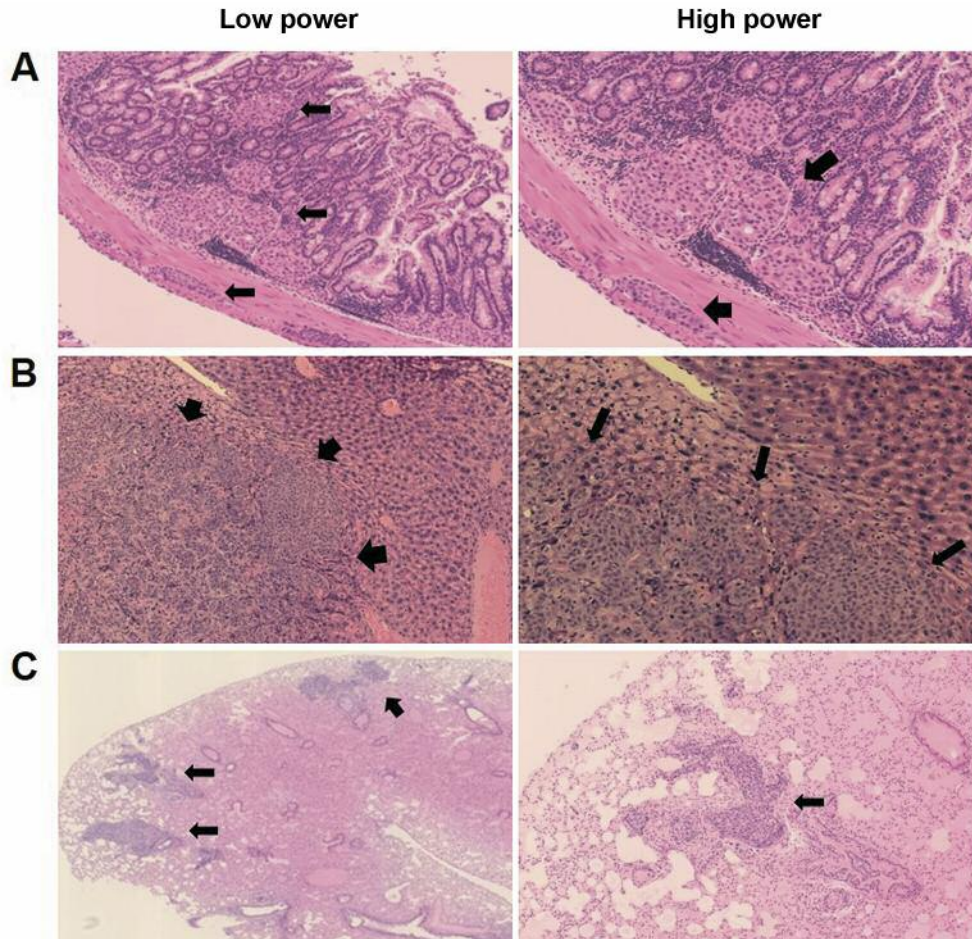


Figure 6. Microscopic findings for the surgical orthotopic implantation model as shown by hematoxylin and eosin staining. A: Orthotopically implanted tumor (arrow) invading the muscularis propria, submucosal, and mucosal layers of colon ($\times 20$ and $\times 40$). Metastatic carcinomas (arrows) in B: liver ($\times 40$ and $\times 100$) and C: lungs ($\times 20$ and $\times 40$).

in a mouse orthotopically implanted with HCT116 (Figure 5A), and peritoneal seeding in the small bowel mesentery (Figure 5B). The livers had multiple whitish nodular metastases (Figure 5C), and the lungs also had whitish nodular metastases (Figure 5D). Microscopic examination of samples from the SOIM group showed that the orthotopically implanted HCT116 cells had infiltrated the *muscularis propria*, submucosal, and mucosal layers of the mouse colon, very similar to the patterns observed for primary human CRC lesions (Figure 6A). Livers (Figure 6B) and lungs (Figure 6C) from the SOIM group were infiltrated by metastatic HCT116 cells, similar to human CRC metastasis.

MACC1 expression in the colon cancer cell lines. Multiple human colon cancer cell lines were selected because of their well-known characteristics of original staging and differentiation, and varied metastatic behavior. qRT-PCR showed that *MACC1* gene was expressed in all the studied

cell lines except SW480. Western blot showed that a pattern similar to that shown by qPCR, with high expression of *MACC1* protein in the HT29, LS513, SW620, and WiDr cell lines, while Colo201 and HCT 116 had little expression, and SW480 had no expression (Figure 7A and B).

Clonal dynamics. All hepatic metastases in SIM mice expressed *MACC1*, with significantly greater expression observed in metastatic HCT116 cells than in the original HCT116 cells ($p < 0.001$; Figure 8A and B). The metastases in the liver showed strong positivity for *MACC1* by immunohistochemistry (Figure 8C and D).

Discussion

Numerous animal models have been established for CRC research. The ideal model should mimic all aspects of metastatic development in humans but metastasis and other

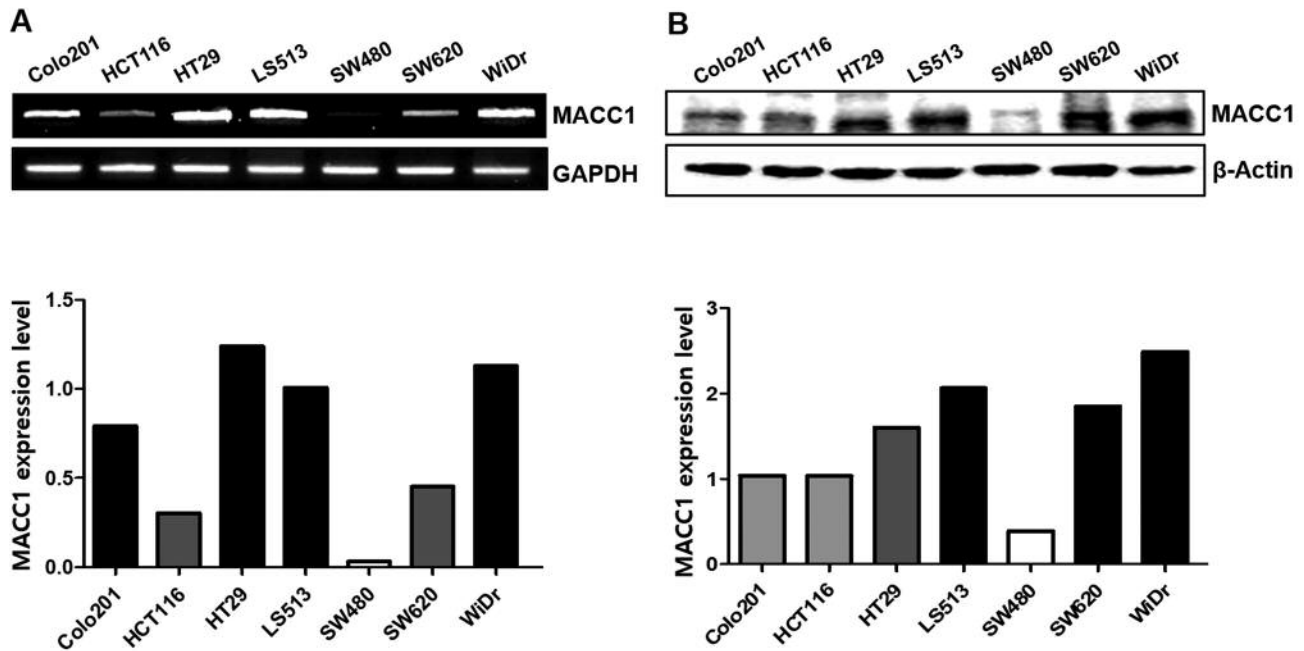


Figure 7. Expression of MET transcriptional regulator *MACC1* (*MACC1*) in colon cancer cell lines. A: Quantitative reverse transcription polymerase chain reaction was performed to determine the *MACC1* expression level. The *MACC1* gene was expressed in Colo201, HCT116, HT29, LS513, SW620 and WiDr cells but not in SW-480 cells. Glyceraldehyde 3-phosphate dehydrogenase (*GAPDH*) was used as an internal control and for relative quantitative measurement of *MACC1* expression. B: Western blot showed that a similar pattern of expression of *MACC1* protein, with high expression in the HT29, LS513, SW620 and WiDr cell lines, while Colo201 and HCT116 had little expression and SW480 no expression in. β -Actin was used as control.

patterns are not uniform and reproducible among models because of differences in the inoculation method, mouse strain and age, cancer cell line, and laboratory conditions. The present study was conducted to compare the SIM and SOIM, which are well-established mouse models of CRC metastasis to liver. Both groups consisted of mice aged exactly 6 weeks because differences in natural killer cell-mediated cytotoxicity between young and old nude mice can affect the implantation and metastasis of human cancer cells (17). The HCT116 cell line was chosen as the human colon cancer cell line for comparison because it has shown high motility and invasive potential in *in vitro* studies, and has been found to be highly tumorigenic in *in vivo* subcutaneous xenograft studies (18, 19). The HCT116 cell line has also been well established as an orthotopic model with cecal injection of cell suspensions or surgical cecal implantation of two 1-mm³ pieces of xenograft (20, 21).

A shorter observation time in an animal model for metastasis study means that experiments can be completed more rapidly. In the present study, the mean observation times until the occurrence of cachexia were 33 and 41 days in the SIM and SOIM, respectively. Giavazzi *et al.* reported the detection of extensive liver metastases in nude mice 30 days after intrasplenic implantation of cancer cells from a

liver tumor (22). Rajput *et al.* studied the orthotopic model with HCT116 cells and found that animals were cachectic 6–8 weeks after implantation, as evidenced by green fluorescent protein imaging after 4 weeks (21). According to Fidler (23), the sequential steps in the pathogenesis of cancer metastasis are progressive growth of the primary cancer, vascularization, invasion, detachment, embolization, survival in circulation, arrest, extravasation, and progressive growth at the metastatic site. Epithelial–mesenchymal transition (EMT) is the essential step for the dissemination of a single cancer cell from the site of a primary tumor (24). The SOIM requires the completion of all steps of metastatic pathogenesis, whereas the SIM does not require EMT at the primary site, suggesting that it requires less time for hepatic metastasis relative to the SOIM.

The rates of liver metastasis were 10/13 in the SIM group and 5/13 in the SOIM group in this study. Many studies in which the splenic injection method was used with various cancer cells have yielded hepatic metastasis rates of 70–100% (9–11, 25, 26). In contrast, many well-established studies in which orthotopic implantation was used have yielded rates of 0–100%, indicating variability according to cancer origin from the primary and metastatic sites, and the number of implanted tumor pieces (21, 27–30). Moreover,

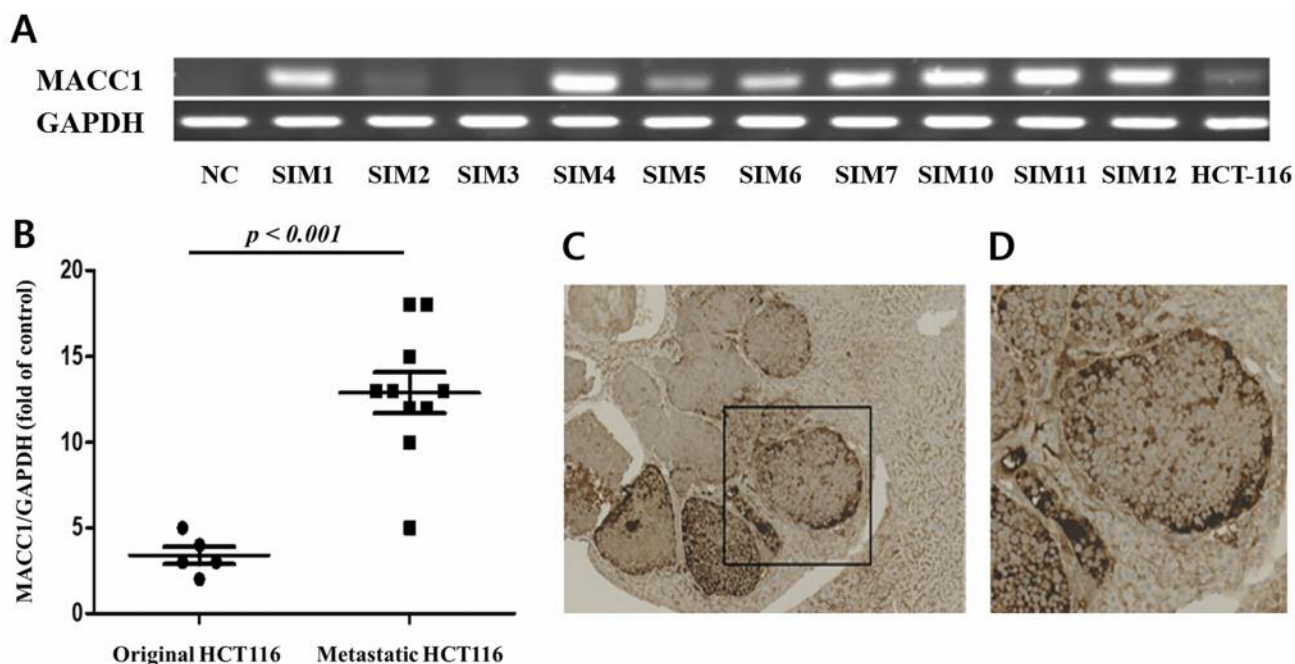


Figure 8. Expression of MET transcriptional regulator MACC1 (MACC1) in the splenic injection model (SIM). Quantitative reverse transcription polymerase chain reaction was performed to determine the expression level of MACC1 in metastases and the HCT116 cell line. Glyceraldehyde 3-phosphate dehydrogenase (GAPDH) was used as an internal control and for relative quantitative measurement of MACC1 expression. A: Almost all hepatic metastases expressed MACC1 gene. B: MACC1 gene expression was significantly greater in metastatic HCT116 cells than in the original HCT116 cells, indicating clonal dynamics during metastasis. C: Metastatic tumor (inset shown in D) in the liver showed strong positive immunohistochemical staining for MACC1 ($\times 40$ and $\times 100$). NC, Normal control.

recent studies of the SOIM established with HCT116 cells yielded liver metastasis rates of 0-67% (21, 29-31). In the present study, the hepatic metastasis rate was significantly greater in the SIM than in the SOIM, with use of the same HCT116 cell line and nude mice of the same age. Thus, the difference in the metastasis rate is definitely attributable to the inoculation method. With the splenic method, almost all cancer cells are thought to enter the portal vein through the splenic vein and become inoculated into the liver parenchymal capillary beds; with the cecal implantation method, only a small proportion of the cancer cells undergo EMT and enter the portal vein through the mesenteric vein.

Numerous novel drugs for CRC treatment have been screened using the PDX model, but the heterogeneity and clonal dynamics of cancer and its microenvironment have been reported as limitations of this model (16). We investigated the heterogeneity and clonal dynamics of metastatic tumors with MACC1 expression levels different from the original cancer cells. MACC1 is a newly identified key regulatory gene of the hepatocyte growth factor-MET signaling, which can predict colon cancer metastasis (32). MACC1 expression has been tested in several well-established human cancer cell lines (33). Almost all Duke C-staged or poorly differentiated colon

cancer cell lines, including Colo201, HCT116, HT29, LS513, SW620 and WiDr, express MACC1, but the Duke B-staged SW480 cell line does not. Stein *et al.* reported that MACC1 is expressed in SW620 but not SW480 cells (32), which our experimental results are in agreement with. We identified MACC1 expression in the original HCT116 cells and in HCT116 SIM metastases. Interestingly, the metastases had significantly greater MACC1 expression than did the original cells, indicating that the HCT116 clone had changed during metastasis from the original clone, which expressed a small amount of MACC1, to a metastatic clone, which expressed a larger amount of MACC1. Thus, the splenic injection of cancer cells resulted in HCT116 clonal dynamics in which metastasis progressed through hematogenous spread.

The limitations of this study were the inclusion of a small number of cases in each group and the use of a single gene to compare clonal dynamics in a single cancer cell line, which may have produced selection bias. Further research should be performed to identify more characteristics and mechanisms of heterogeneity and clonal dynamics during hematogenous spread in the SIM, as well as changes during EMT in the SOIM, which were not analyzed in this study because of the small number of metastases that occurred.

In summary, the SIM for colon cancer cells had a shorter observation time and greater rate of hepatic metastasis than did the SOIM, and was very efficient and practical. Clonal dynamics were also identified in the SIM. However, the SOIM should also be considered for the development of novel drugs to inhibit metastasis because this model mimics the full steps of EMT and metastasis of human CRC.

Conflicts of Interest

The Authors report no proprietary or commercial interest in any product mentioned or concept discussed in this article.

Authors' Contributions

S.H.K and K.B.B designed and performed the experiment; M.S.K performed the experiment; D.H.K supervised the experiments

Acknowledgements

This research was supported by a 2018 Research Grant from Inje University Busan Paik Hospital to K.B.B.

References

- 1 Siegel RL, Miller KD and Jemal A: Cancer statistics, 2015. *CA Cancer J Clin* 65: 5-29, 2015. PMID: 25559415. DOI: 10.3322/caac.21254
- 2 Manfredi S, Lepage C, Hatem C, Coatmeur O, Faivre J and Bouvier AM: Epidemiology and management of liver metastases from colorectal cancer. *Ann Surg* 244: 254-259, 2006. PMID: 16858188. DOI: 10.1097/01.sla.0000217629.94941.cf
- 3 Markowitz SD and Bertagnolli MM: Molecular origins of cancer: Molecular basis of colorectal cancer. *N Engl J Med* 361: 2449-2460, 2009. PMID: 20018966. DOI: 10.1056/NEJMra0804588
- 4 Tournigand C, Andre T, Achille E, Lledo G, Flesh M, Mery-Mignard D, Quinaux E, Couteau C, Buyse M, Ganem G, Landi B, Colin P, Louvet C and de Gramont A: FOLFIRI followed by FOLFOX6 or the reverse sequence in advanced colorectal cancer: A randomized GERCOR study. *J Clin Oncol* 22: 229-237, 2004. PMID: 14657227. DOI: 10.1200/JCO.2004.05.113
- 5 Saltz LB, Clarke S, Diaz-Rubio E, Scheithauer W, Figer A, Wong R, Koski S, Lichinitser M, Yang TS, Rivera F, Couture F, Sirzen F and Cassidy J: Bevacizumab in combination with oxaliplatin-based chemotherapy as first-line therapy in metastatic colorectal cancer: A randomized phase III study. *J Clin Oncol* 26: 2013-2019, 2008. PMID: 18421054. DOI: 10.1200/JCO.2007.14.9930
- 6 Bennouna J, Sastre J, Arnold D, Osterlund P, Greil R, Van Cutsem E, von Moos R, Vieitez JM, Bouche O, Borg C, Steffens CC, Alonso-Orduna V, Schlichting C, Reyes-Rivera I, Bendahmane B, Andre T, Kubicka S and ML18147 Study Investigators: Continuation of bevacizumab after first progression in metastatic colorectal cancer (ML18147): A randomised phase 3 trial. *Lancet Oncol* 14: 29-37, 2013. PMID: 23168366. DOI: 10.1016/S1470-2045(12)70477-1
- 7 Van Cutsem E, Kohne CH, Hitre E, Zaluski J, Chang Chien CR, Makhson A, D'Haens G, Pinter T, Lim R, Bodoky G, Roh JK, Folprecht G, Ruff P, Stroh C, Tejpar S, Schlichting M, Nippgen J and Rougier P: Cetuximab and chemotherapy as initial treatment for metastatic colorectal cancer. *N Engl J Med* 360: 1408-1417, 2009. PMID: 19339720. DOI: 10.1056/NEJMoa0805019
- 8 Tentler JJ, Tan AC, Weekes CD, Jimeno A, Leong S, Pitts TM, Arcaroli JJ, Messersmith WA and Eckhardt SG: Patient-derived tumour xenografts as models for oncology drug development. *Nat Rev Clin Oncol* 9: 338-350, 2012. PMID: 22508028. DOI: 10.1038/nrclinonc.2012.61
- 9 Garofalo A, Chirivi RG, Scanziani E, Mayo JG, Vecchi A and Giavazzi R: Comparative study on the metastatic behavior of human tumors in nude, beige/nude/XID and severe combined immunodeficient mice. *Invasion Metastasis* 13: 82-91, 1993. PMID: 8225855.
- 10 Kozlowski JM, Fidler IJ, Campbell D, Xu ZL, Kaighn ME and Hart IR: Metastatic behavior of human tumor cell lines grown in the nude mouse. *Cancer Res* 44: 3522-3529, 1984. PMID: 6744277.
- 11 Naito S, Giavazzi R, Walker SM, Itoh K, Mayo J and Fidler IJ: Growth and metastatic behavior of human tumor cells implanted into nude and beige nude mice. *Clin Exp Metastasis* 5: 135-146, 1987. PMID: 3594971. DOI: 10.1007/bf00058059
- 12 Goldrosen MH, Paolini N, Jr and Holyoke ED: Description of a murine model of experimental hepatic metastases. *J Natl Cancer Inst* 77: 823-828, 1986. PMID: 3462419. DOI: 10.1093/jnci/77.3.823
- 13 de Jong GM, Aarts F, Hendriks T, Boerman OC and Bleichrodt RP: Animal models for liver metastases of colorectal cancer: Research review of preclinical studies in rodents. *J Surg Res* 154: 167-176, 2009. PMID: 18694579. DOI: 10.1016/j.jss.2008.03.038
- 14 Rashidi B, Gamagami R, Sasson A, Sun FX, Geller J, Moossa AR and Hoffman RM: An orthotopic mouse model of metastasis of human colon cancer liver metastasis. *Clin Cancer Res* 6: 2556-2561, 2000. PMID: 10873112.
- 15 Greaves M and Maley CC: Clonal evolution in cancer. *Nature* 481: 306-313, 2012. PMID: 22258609. DOI: 10.1038/nature10762
- 16 Cassidy JW, Caldas C and Bruna A: Maintaining tumor heterogeneity in patient-derived tumor xenografts. *Cancer Res* 75: 2963-2968, 2015. PMID: 26180079. DOI: 10.1158/0008-5472.CAN-15-0727
- 17 Hanna N: Expression of metastatic potential of tumor cells in young nude mice is correlated with low levels of natural killer cell-mediated cytotoxicity. *Int J Cancer* 26: 675-680, 1980. PMID: 6972360. DOI: 10.1002/ijc.2910260521
- 18 Sawhney RS, Zhou GH, Humphrey LE, Ghosh P, Kreisberg JI and Brattain MG: Differences in sensitivity of biological functions mediated by epidermal growth factor receptor activation with respect to endogenous and exogenous ligands. *J Biol Chem* 277: 75-86, 2002. PMID: 11684674. DOI: 10.1074/jbc.M103268200
- 19 Wang J, Sun L, Myeroff L, Wang X, Gentry LE, Yang J, Liang J, Zborowska E, Markowitz S and Willson JK: Demonstration that mutation of the type II transforming growth factor beta receptor inactivates its tumor suppressor activity in replication error-positive colon carcinoma cells. *J Biol Chem* 270: 22044-22049, 1995. PMID: 7665626. DOI: 10.1074/jbc.270.37.22044
- 20 Ishizu K, Sunose N, Yamazaki K, Tsuruo T, Sadahiro S, Makuuchi H and Yamori T: Development and characterization of a model of liver metastasis using human colon cancer HCT116 cells. *Biol Pharm Bull* 30: 1779-1783, 2007. PMID: 17827739. DOI: 10.1248/bpb.30.1779

- 21 Rajput A, Dominguez San Martin I, Rose R, Beko A, Levea C, Sharratt E, Mazurchuk R, Hoffman RM, Brattain MG and Wang J: Characterization of HCT116 human colon cancer cells in an orthotopic model. *J Surg Res* 147: 276-281, 2008. PMID: 17961596. DOI: 10.1016/j.jss.2007.04.021
- 22 Giavazzi R, Jessup JM, Campbell DE, Walker SM and Fidler IJ: Experimental nude mouse model of human colorectal cancer liver metastases. *J Natl Cancer Inst* 77: 1303-1308, 1986. PMID: 3467119.
- 23 Fidler IJ: The pathogenesis of cancer metastasis: The 'seed and soil' hypothesis revisited. *Nat Rev Cancer* 3: 453-458, 2003. PMID: 12778135. DOI: 10.1038/nrc1098
- 24 Thiery JP: Epithelial-mesenchymal transitions in tumour progression. *Nat Rev Cancer* 2: 442-454, 2002. PMID: 12189386. DOI: 10.1038/nrc822
- 25 Giavazzi R, Campbell DE, Jessup JM, Cleary K and Fidler IJ: Metastatic behavior of tumor cells isolated from primary and metastatic human colorectal carcinomas implanted into different sites in nude mice. *Cancer Res* 46: 1928-1933, 1986. PMID: 3948174.
- 26 Morikawa K, Walker SM, Jessup JM and Fidler IJ: *In vivo* selection of highly metastatic cells from surgical specimens of different primary human colon carcinomas implanted into nude mice. *Cancer Res* 48: 1943-1948, 1988. PMID: 3349467.
- 27 Fu XY, Besterman JM, Monosov A and Hoffman RM: Models of human metastatic colon cancer in nude mice orthotopically constructed by using histologically intact patient specimens. *Proc Natl Acad Sci USA* 88: 9345-9349, 1991. PMID: 1924398. DOI: 10.1073/pnas.88.20.9345
- 28 Furukawa T, Kubota T, Watanabe M, Kuo TH, Nishibori H, Kase S, Saikawa Y, Tanino H, Teramoto T and Ishibiki K: A metastatic model of human colon cancer constructed using cecal implantation of cancer tissue in nude mice. *Surg Today* 23: 420-423, 1993. PMID: 8324335. DOI: 10.1007/bf00309500
- 29 Flatmark K, Maelandsmo GM, Martinsen M, Rasmussen H and Fodstad O: Twelve colorectal cancer cell lines exhibit highly variable growth and metastatic capacities in an orthotopic model in nude mice. *Eur J Cancer* 40: 1593-1598, 2004. PMID: 15196545. DOI: 10.1016/j.ejca.2004.02.023
- 30 Cespedes MV, Espina C, Garcia-Cabezas MA, Trias M, Boluda A, Gomez del Pulgar MT, Sancho FJ, Nistal M, Lacal JC and Manges R: Orthotopic microinjection of human colon cancer cells in nude mice induces tumor foci in all clinically relevant metastatic sites. *Am J Pathol* 170: 1077-1085, 2007. PMID: 17322390. DOI: S0002-9440(10)60926-1
- 31 Chen HJ, Yang BL, Chen YG, Lin Q, Zhang SP and Gu YF: A GFP-labeled human colon cancer metastasis model featuring surgical orthotopic implantation. *Asian Pac J Cancer Prev* 13: 4263-4266, 2012. PMID: 23167325. DOI: 10.7314/apjcp.2012.13.9.4263
- 32 Stein U, Walther W, Arlt F, Schwabe H, Smith J, Fichtner I, Birchmeier W and Schlag PM: MACC1, a newly identified key regulator of HGF-MET signaling, predicts colon cancer metastasis. *Nat Med* 15: 59-67, 2009. PMID: 19098908. DOI: 10.1038/nm.1889
- 33 Schneider M, Huber J, Hadaschik B, Siegers GM, Fiebig HH and Schuler J: Characterization of colon cancer cells: a functional approach characterizing CD133 as a potential stem cell marker. *BMC Cancer* 12: 96, 2012. PMID: 22433494. DOI: 10.1186/1471-2407-12-96

Received April 18, 2020

Revised April 30, 2020

Accepted May 4, 2020